ORIGINAL ARTICLE

Circulating Plasma Extracellular Microvesicle MicroRNA Cargo and Endothelial Dysfunction in Children with Obstructive Sleep Apnea

Abdelnaby Khalyfa[1]*, Leila Kheirandish-Gozal[1]*, Ahamed A. Khalyfa[1], Mona F. Philby[1‡], María Luz Alonso-Álvarez[2], Meelad Mohammadi[1], Rakesh Bhattacharjee[1§], Joaquin Terán-Santos[2], Lei Huang[3], Jorge Andrade[3], and David Gozal[1]

[1]Section of Sleep Medicine, Department of Pediatrics, Pritzker School of Medicine, Biological Sciences Division, and [3]Center for Research Informatics, The University of Chicago, Chicago, Illinois; and [2]Sleep Unit, CIBER of Respiratory Diseases, Instituto Carlos III, CIBERES, Hospital Universitario de Burgos, Burgos, Spain

ORCID IDs: 0000-0003-3332-1057 (L.K.-G.); 0000-0001-8195-6036 (D.G.).

Abstract

Rationale: Obese children are at increased risk for developing obstructive sleep apnea (OSA), and both of these conditions are associated with an increased risk for endothelial dysfunction (ED) in children, an early risk factor for atherosclerosis and cardiovascular disease. Although weight loss and treatment of OSA by adenotonsillectomy improve endothelial function, not every obese child or child with OSA develops ED. Exosomes are circulating extracellular vesicles containing functional mRNA and microRNA (miRNA) that can be delivered to other cells, such as endothelial cells.

Objectives: To investigate whether circulating exosomal miRNAs of children with OSA differentiate based on endothelial functional status.

Methods: Obese children (body mass index *z* score >1.65) and nonobese children were recruited and underwent polysomnographic testing (PSG), and fasting endothelial function measurements and blood draws in the morning after PSG. Plasma exosomes were isolated from all subjects. Isolated exosomes were then incubated with confluent endothelial cell monolayer cultures. Electric cell-substrate impedance sensing systems were used to determine the ability of exosomes to disrupt the intercellular barrier formed by confluent endothelial cells. In addition, immunofluorescent assessments of zonula occludens-1 tight junction protein cellular distribution were conducted to examine endothelial barrier dysfunction. miRNA and mRNA arrays were also applied to exosomes and endothelial cells, and miRNA inhibitors and mimics were transfected for mechanistic assays.

Measurements and Main Results: Plasma exosomes isolated from either obese children or nonobese children with OSA were primarily derived from endothelial cell sources and recapitulated ED, or its absence, in naive human endothelial cells and also *in vivo* when injected into mice. Microarrays identified a restricted signature of exosomal miRNAs that readily distinguished ED from normal endothelial function. Among the miRNAs, expression of exosomal miRNA-630 was reduced in children with ED and normalized after therapy along with restoration of endothelial function. Conversely, transfection of exosomes from subjects without ED with an miRNA-630 inhibitor induces the ED functional phenotype. Gene target discovery experiments further revealed that miRNA-630 regulates 416 gene targets in endothelial cells that include the Nrf2, AMP kinase, and tight junction pathways.

Conclusions: These observations elucidate a novel role of exosomal miRNA-360 as a putative key mediator of vascular function and cardiovascular disease risk in children with underlying OSA and/or obesity, and identify therapeutic targets.

Keywords: sleep apnea; inflammation; obesity; intermittent hypoxia; endothelial function

(Received in original form February 15, 2016; accepted in final form April 20, 2016)

*These authors contributed equally to the work.

‡Present affiliation: Department of Pediatrics, King Saud School of Medicine, Riyadh, Kingdom of Saudi Arabia.

§Present affiliation: Department of Pediatrics, University of California at San Diego, San Diego, California.

Supported by the Herbert T. Abelson Chair of Pediatrics (D.G. and L.K.-G.), National Institutes of Health grant HL130984 (L.K.-G.), a Scientist Development grant from the American Heart Association 3SDG14780079 (R.B.), a Fellowship Educational grant award from the Kingdom of Saudi Arabia (M.F.P.), and Spanish Respiratory Society and Mutua Madrileña grants (M.L.A.-Á. and J.T.-S.).

This article has an online supplement, which is accessible from this issue's table of contents at www.atsjournals.org

Am J Respir Crit Care Med Vol 194, Iss 9, pp 1116–1126, Nov 1, 2016

Originally Published in Press as DOI: 10.1164/rccm.201602-0323OC on May 10, 2016
Internet address: www.atsjournals.org

At a Glance Commentary

Scientific Knowledge on the Subject: Obstructive sleep apnea and obesity are independently associated with an increased risk for endothelial dysfunction in children. However, not every child with either one of these two conditions is affected.

What This Study Adds to the Field: A selective cluster of plasma-derived exosomal microRNAs readily differentiates between normal and abnormal endothelial function in children with obstructive sleep apnea or obesity, and recapitulates such vascular phenotype both *in vitro* and in mice.

Obesity is a frequent condition in children that carries a substantial risk for cardiovascular disease (CVD) later in life (1–3). Similarly, obstructive sleep apnea (OSA) is a highly prevalent pediatric disorder typically associated with a higher risk for future cardiovascular morbidity, primarily presenting as increased systemic blood pressure deregulation that can lead to ventricular remodeling, and altered endothelial function, an early precursor of atherosclerosis, the latter being improved by treatment of OSA with adenotonsillectomy (Tx) (4–7). Furthermore, obese children (OB) are at significantly higher risk for OSA (8). However, not every child, even with severe OSA or obesity, displays abnormal endothelial function (9–11). To date, the mechanisms underlying the determinants of CVD susceptibility remain unclear (12).

Intercellular communication is an essential hallmark of multicellular organisms and can be mediated through direct cell–cell contact or transfer of secreted vesicles (13, 14). Exosomes are 30- to 100-nm vesicular structures that contain a wide variety of proteins, lipids, RNAs, nontranscribed RNAs, microRNAs (miRNAs), and small RNAs. These diverse cargos allow exosomes to provide unique opportunities for biomarker discovery and development of noninvasive diagnostics when examined in biologic fluids, such as urine and blood plasma, and formulation of novel therapies (5, 11, 13, 15–21).

In this study, we hypothesized that plasma-derived exosomes from either OB or children with OSA with evidence of endothelial dysfunction (ED) exert differential effects on endothelial cell monolayer impedance, tight-junction function, and expression of adhesion molecules when compared with either OB or children with OSA with normal endothelial function (NEF). We also explored whether the standard treatment for OSA in children, surgical Tx, reverses exosome-induced changes. In addition, we examined whether exosomal miRNA cargo differences are present between children with ED and children with NEF, and whether such miRNA differences may underlie the mechanisms accounting for the presence of ED.

Methods

Detailed descriptions of subjects, reagents, cell culture, exosome isolation, electron microscopy, confocal fluorescence microscopy, Western blot analysis, isolation, and analysis of miRNA experiments are provided in the METHODS section in the online supplement.

Subjects

The study was approved by the human subject committee of each of the participating centers (University of Chicago institutional review board protocol #09-115-B and Comité Ético de Investigación Clínica del Área de Salud de Burgos y Soria protocol # 603), and informed consent was obtained from the legal caregiver of each participant. Consecutive healthy obese or nonobese prepubertal children (ages 4–12 yr) from the community, and children being evaluated for habitual snoring who were polysomnographically diagnosed with OSA were invited to participate. All participants underwent baseline anthropometric and blood pressure assessments, and overnight polysomnography, which were interpreted using standard approaches.

Endothelial Function Test in Children

Measurements of endothelial function followed by a fasting blood draw were performed in the morning (*see* METHODS section in the online supplement). The time to maximal regional blood flow after occlusion release (T_{max}) is representative of the postocclusion hyperemic response, an index of nitric oxide (NO)-dependent endothelial function (9, 22). T_{max} greater than 45 seconds was considered indicative of abnormal endothelial function (15).

According to our recruitment strategies, five distinctly different groups of children were identified: controls subjects (healthy nonsnoring children with normal polysomnographic test, body mass index [BMI] z score <1.34, and normal T_{max}); OB (i.e., BMI z score $\geqslant 1.65$ but normal polysomnographic test with normal T_{max} [OB_{NEF}] or abnormal T_{max} [B_{ED}]); snoring children with abnormal polysomnographic findings confirming the presence of OSA (*see* METHODS section in the online supplement), BMI z score less than or equal to 1.65; and either normal T_{max} (OSA_{NEF}) or abnormal T_{max} (OSA_{ED}). Exclusion criteria are described in the METHODS section in the online supplement.

Exosome Isolation, Labeling, and Characterization

Exosomes were isolated from plasma using a commercially available kit (Life Technologies, Carlsbad, CA) and carefully characterized (*see* METHODS section in the online supplement). Exosomes isolated from OB or children with OSA with or without ED were intravenously injected into mice or applied to endothelial cells *in vitro*. Purified exosomes from ED and

Author Contributions: A.K. conceptualized parts of the study, performed experiments, analyzed data, and drafted components of the manuscript. L.K.-G. conceptualized the study, performed experiments, coordinated the database, was responsible for sleep study interpretation, performed data analyses, and edited the manuscript. A.A.K., M.F.P., M.L.A.-Á., M.M., R.B., and J.T.-S. collected data and contributed to manuscript editing. L.H. and J.A. performed bioinformatics analyses. D.G. conceptualized the study, analyzed data, and drafted portions of the manuscript.

Correspondence and requests for reprints should be addressed to David Gozal, M.D., Section of Pediatric Sleep Medicine, Department of Pediatrics, Pritzker School of Medicine, The University of Chicago, KCBD, Room 4100, 900 East 57th Street, Mailbox 4, Chicago, IL 60637-1470. E-mail: dgozal@uchicago.edu

NEF were subjected to Amnis-ImageStream cytometer (Millipore/Amnis, Seattle, WA) for detection of their cell sources (*see* METHODS section in the online supplement).

Primary Endothelial Cell Culture

Human microvascular endothelial cells (always used before passage 4–6) were purchased from Lonza (catalog #CC-2543; Allendale, NJ) and grown in Dulbecco's modified Eagle medium supplemented and incubated at 37°C and 5% CO_2.

Electric Cell-Substrate Impedance Sensing and Imunofluorescence

To examine the effect of exosomes on endothelial cell monolayer barrier, endothelial cells were grown to confluence into electric cell-substrate impedance sensing (ECIS) arrays as a single confluent monolayer. Exosomes were added in duplicate wells and monitored in the ECIS instrument (Applied Biophysics Inc., Troy, NY) for up to 24 hours (23, 24). The baseline was established using culture medium (300 μl/well) alone and compared with values obtained using electrodes covered with a monolayer of cells in 500-μl medium.

For immunofluorescence staining, confluent endothelial cell monolayers were grown on cover slips for 12-well plates, after which isolated exosomes from subjects were added individually to cover slips for 24 hours. Cells were fixed, permeabilized, and followed by overnight incubation at 4°C with the tight junction protein zonula occludens (ZO)-1, and vascular endothelial-cadherin (Life Technologies, Grand Island, NY), and the adhesion molecules intercellular adhesion molecule-1 and vascular cell adhesion molecule-1 (Santa Cruz Biotechnology, Inc., Dallas, TX). Images were captured with a Leica SP5 Tandem Scanner Spectral 2-photon confocal microscope (Leica Microsystems, Inc., Buffalo Grove, IL) with a 63 × oil-immersion lens.

Western Blot Analysis

Lysates of cells and exosomes were separated by sodium dodecyl sulfate/polyacrylamide gel electrophoresis, transferred to polyvinylidene difluoride membranes, and incubated with antibodies as described in the METHODS section in the online supplement.

miRNA Isolation and Microarrays

Total RNA including miRNA was isolated from exosomes using miRNeasy Mini Kit-column-based system following the manufacturer's instructions (Qiagen, Valencia, CA) and profiled on 2006 Agilent human miRNA Microarray (Agilent Technologies, Santa Clara, CA). Array were hybridized, washed, and scanned with Agilent microarray scanner. The results were extracted using Agilent Feature Extraction software (v12.0). A feature was listed as detectable if greater than 50% of the signals in at least one of the two groups were above the detection limit ("well above background" flag = 1) and a probe was considered to be detectable if greater than 50% of the replicated features were detectable.

Gene Ontology and Functional Annotation

Analysis of gene ontology annotation was performed by applying Database for Annotation, Visualization and Integrated Discovery functional annotation tool (DAVID 6.7; http://david.abcc.ncifcrf.gov/). Molecular targets for each miRNA were retrieved and the validated miRNA-target interaction network was obtained from the CyTargetLinker plugin in the Cytoscape environment (25). The network containing interactions between differentially expressed miRNA and putative targets was constructed and visualized using Cytoscape (http://cytoscape.org) (26).

miRNA Mimics and Inhibitors *In Vitro* and *In Vivo*

Exosome transfections were performed using the Exo-Fect Exosome Transfection Reagent as described by the manufacturer's protocol (cat# EXFT20A-1; System Biosciences, Inc., Mountain View, CA). The transfected exosome pellets were suspended in 300 μl 1 × phosphate buffered saline, and used in the ECIS system for the miRNA mimics and inhibitors of interest (75 μl were added to approximately 5×10^5 cells/well in a 12-well culture plate grown in exosome-depleted fetal bovine serum), and reaching equivalent exosome concentrations across conditions (27–30). miRNA mimics and inhibitors were purchased from Life Technologies (Grand Island, NY). The specifically desired increase or decrease in miRNA-630 content was verified using reverse-transcriptase polymerase chain reaction (RT-PCR).

Data Analyses

Results are presented as means ± SD, unless stated otherwise. All numerical data were subjected to statistical analysis using independent Student's *t* tests or analysis of variance followed by *post hoc* tests (Tukey) as appropriate. Chi-square analysis was performed on categorical data concerning demographic characteristics of the various groups. Pearson correlation testing was conducted to establish association between several study parameters, including ECIS-derived normalized resistance changes and T_{max} in endothelial function tests. Finally, canonical correlation analyses were performed to explore the relationships between sets of variables. Statistical analyses were performed using SPSS version 21.0 (SPPS Inc., Chicago, IL). For all comparisons, a two-tailed *P* less than 0.05 was considered to define statistical significance.

Results

Subject Characteristics

A total of 128 children completed the study. Their demographic and polysomnographic characteristics are provided in Table 1. There were no significant differences in age, sex, and ethnicity among the two OSA subgroups, but the OSA_{ED} children showed slightly higher BMI *z* scores than OSA_{NEF}, and both OSA groups had higher BMI *z* scores compared with control children (CO) (Table 1). No differences in BMI *z* scores were present in OB_{ED} and OB_{NEF}. There were no significant differences in the severity of OSA, as indicated by either the obstructive apnea–hypopnea index or the nadir oxygen saturation as measured by pulse oximetry levels, in systolic and diastolic blood pressures, or in lipid profiles between OSA_{ED} and OSA_{NEF} children, but these measures were significantly different from CO children, suggesting increased risk for CVD in all subjects independent of their ED or NEF status (Table 1).

As anticipated from the definition of ED, both OB_{ED} and OSA_{ED} groups had markedly prolonged T_{max} (56.8 ± 8.6 s and 54.7 ± 8.5 s), compared with OB_{NEF} (33.2 ± 7.3 s; $P < 0.01$), OSA_{NEF} (31.6 ± 6.2 s; $P < 0.01$), or CO (29.9 ± 5.1 s; $P < 0.01$). A subset of 16 OSA_{ED} children was treated with the standard clinically recommended approach consisting in surgical removal of tonsils and adenoids, and underwent a second assessment as per

Table 1. General Characteristics of Obese Children and Children with OSA with and without Endothelial Dysfunction and Healthy Control Subjects

	OB_{NEF} ($n = 23$)	OB_{ED} ($n = 20$)	OSA_{NEF} ($n = 34$)	OSA_{ED} ($n = 25$)	Control ($n = 26$)
Age, yr	7.6 ± 2.6	7.7 ± 2.8	7.3 ± 2.4	7.4 ± 2.3	7.3 ± 2.2
Sex, male, %	56.5	60	50	56	58
Ethnicity, white, n	6	6	11	9	8
BMI *z* score	1.74 ± 0.28*	1.76 ± 0.31*	1.37 ± 0.22	1.42 ± 0.27†	1.08 ± 0.21†
Systolic blood pressure					
mm Hg	113.2 ± 8.6	114.0 ± 9.1	108.2 ± 8.4	112.8 ± 9.2†	102.3 ± 8.4†
z score	1.46 ± 0.21†	1.44 ± 0.23†	1.22 ± 0.19	1.38 ± 0.24†	1.06 ± 0.20†
Diastolic blood pressure					
mm Hg	68.7 ± 7.9	68.9 ± 8.3	65.8 ± 7.2	67.8 ± 7.8‡	60.9 ± 6.7‡
z score	1.35 ± 0.25†	1.34 ± 0.26†	1.27 ± 0.27	1.33 ± 0.29†	1.08 ± 0.21†
Obstructive apnea–hypopnea index, events/h	0.9 ± 0.4	0.8 ± 0.6	12.8 ± 8.4	13.1 ± 9.4‡	0.3 ± 0.3‡
Sp_{O_2} nadir, %	93.2 ± 3.3	93.9 ± 4.1	75.9 ± 10.9	73.0 ± 11.9‡	92.1 ± 2.9‡
Total cholesterol, mg/dl	171.6 ± 37.3	173.4 ± 40.0	174.9 ± 36.1	178.3 ± 37.8‡	159.4 ± 19.3‡
HDL cholesterol, mg/dl	48.9 ± 8.7	44.8 ± 9.2	44.7 ± 8.5	46.7 ± 8.8‡	59.3 ± 7.8‡
LDL cholesterol, mg/dl	119.3 ± 19.9	121.8 ± 23.6	117.2 ± 24.5	120.5 ± 24.7‡	95.7 ± 20.3‡
Triglycerides, mg/dl	107.2 ± 32.1	110.3 ± 33.9	105.7 ± 35.5	107.8 ± 36.7†	93.7 ± 28.3†
Time to maximal hyperemic responses, T_{max}; s	33.2 ± 7.3§	56.8 ± 8.6§	31.6 ± 6.2§	54.7 ± 8.5‡§	29.9 ± 5.1‡

Definition of abbreviations: BMI = body mass index; ED = endothelial dysfunction; HDL = high-density lipoprotein; LDL = low-density lipoprotein; NEF = normal endothelial function; OB = obese; OSA = obstructive sleep apnea; Sp_{O_2} = oxygen saturation as measured by pulse oximetry; T_{max} = time to maximal regional blood flow after occlusion release.

*$P < 0.01$ obese children versus all three other groups (OSA and control children).

†$P < 0.05$ versus control subjects.

‡$P < 0.01$ versus control subjects.

§$P < 0.01$ versus corresponding group.

protocol within 4–8 months after surgery (*see* Table E1 in the online supplement) (14). These children showed normalization of their respiratory disturbance during sleep (apnea–hypopnea index decreased from 15.7 ± 4.7/h sleep to 0.7 ± 0.4/h sleep; $P < 0.001$), and in all children but one, normalization of endothelial function occurred (T_{max} decreased from 57.7 ± 8.5 s to 37.8 ± 7.3 s; $P < 0.001$) (*see* Table E1).

Exosome Cellular Sources

The characteristics and properties of isolated exosomes are described in Figure E1. The overall concentrations of plasma-isolated exosomes among children with ED and NEF were similar. However, exosomes from children with ED were increasingly derived from either endothelial cells or endothelial progenitor cells, when compared with those from matched children with NEF (*see* Figure E2), with no significant differences for monocytes, T-cell lymphocytes, or neutrophils. The concentration of exosomes from platelet sources was increased only in children with OSA and ED, but not among OB with ED without OSA. Indeed, children with OSA had overall increased platelet-derived exosomes (852 ± 122/10,000 counts in OSA_{ED}, 367 ± 89/10,000 counts in OSA_{NEF}, 228 ± 78/10,000 counts in either OB_{ED} or OB_{NEF}, and 217 ± 81/10,000 counts in control subjects; $P < 0.01$ OSA_{ED} vs. all other groups).

Exosomal Effects on Endothelial Cell Monolayers

Human primary endothelial cells were exposed to exosomes from NEF and children with ED corresponding to both obese and OSA groups. ECIS normalized resistance values were continuously monitored, and revealed substantial decrements in monolayer resistance among exosomes from children with ED, which were absent or markedly attenuated in children with NEF (Figure 1; $P < 0.001$). Of note, the ECIS array enables assessment of morphologic cell changes, cell locomotion, and other cell events within the cytoskeleton. Notably, ECIS values at either 6 hours (data not shown) or 24 hours were strongly associated with corresponding T_{max} values (Figure 1A). The data presented in Figure 1B show the normalized ECIS resistance values for OB_{ED} compared with OB_{NEF} and control subjects, and revealed substantial decrements in monolayer resistance of OB_{ED} subjects ($P < 0.01$). Similarly, Figure 1C illustrates the normalized ECIS resistance values for OSA_{ED} compared with OSA_{NEF} and CO, which revealed decreases in monolayer resistance of after treatment with OSA_{ED}-derived exosomes ($P < 0.001$). Furthermore, ED-derived exosomes induced disruption of the endothelial cell membrane as illustrated by discontinuity of V-cadherin, altered topographic distribution of the tight junction protein ZO-1, and increased expression of adhesion molecules intercellular adhesion molecule-1 and vascular cell adhesion molecule-1 (Figure 1D; *see* Figure E3). Similarly, ED exosomes from either OSA or OB children, but not NEF exosomes (from OB, OSA, or CO), induced significant reductions in expression of endothelial NO synthase (eNOS) mRNA, when compared with exosomes derived from healthy control subjects (ED, 57.6 ± 8.9% vs. NEF, 2.9 ± 5.2%; $P < 0.001$).

Exosome Delivery and Endothelial Function in Mice

When plasma-derived exosomes isolated from children with ED (either OB or OSA) or NEF (OB, OSA, and control subjects) were intravenously injected into mice, and vascular function was assessed at 24 and 48 hours after injection, significant prolongations in T_{max} occurred after administration of ED-derived exosomes

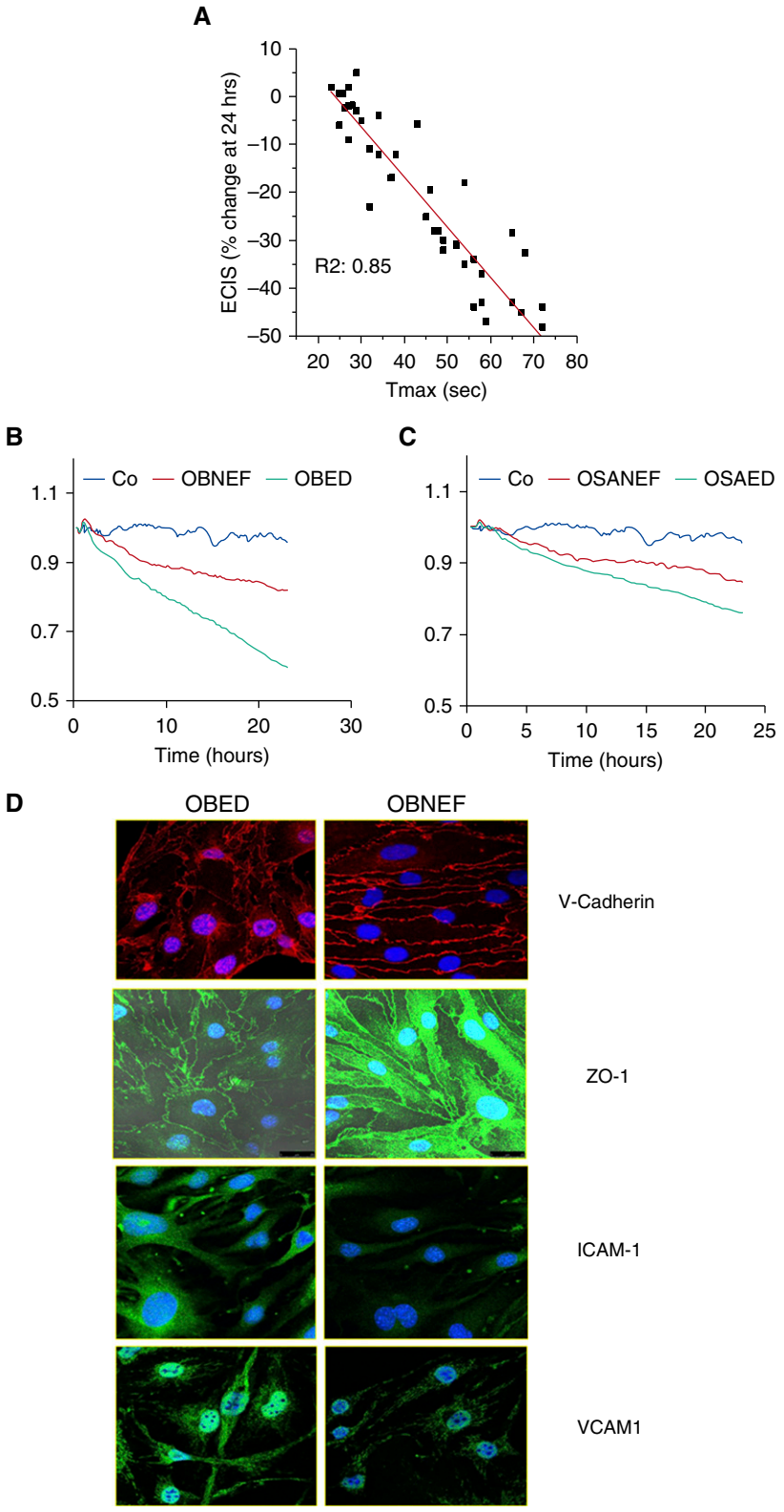

Figure 1. Exosome-mediated *in vitro* effects on endothelial cell monolayer resistance. (*A*) Scattergram of T_{max}, a measure of endothelial function in obese (OB) children or children with obstructive sleep apnea (OSA), plotted against plasma-derived exosome effects on endothelial cell monolayer resistance (ECIS) at 24 hours ($R^2 = 0.85$; $P < 0.0001$; n = 41). (*B*) Ensemble-averaged (both obese and OSA). Such changes were absent after treatment with NEF-derived exosomes when compared with control exosomes (Figure 2). Tx treatment of OSA in the children with ED not only normalized their T_{max}, but also led to normalization of plasma exosome-induced endothelial cell monolayer resistance changes (pre-Tx, $-37.8 \pm 7.4\%$ vs. post-Tx, $-4.7 \pm 4.6\%$; n = 15; $P < 0.001$).

Exosomal Endothelial Cell Uptake and miRNA Cargo

To study the uptake of isolated exosomes, we used a fluorescent dye (Exo-Red) that allows tracking of cellular interaction and uptake by endothelial cells (*see* Figure E4). Differences in miRNA exosomal content between NEF and children with ED were initially explored using miRNA arrays, and revealed a restricted cluster of five miRNAs that were consistently altered across the two groups independent of obese or OSA status, with abundance of four miRNAs being reduced in ED (miRNA-16–5, 3.18-fold, $P < 0.0001$; miRNA-451a, 3.74-fold, $P < 0.0001$; miRNA-5100, 1.65-fold, $P < 0.01$; and miRNA-630, 4.11-fold, $P < 0.0001$) and increased abundance being found for one miRNA (miRNA-4665–3p, 2.35-fold; $P < 0.01$). These findings were subsequently validated and confirmed in all groups (n = 20/group) using RT-PCR. Furthermore, marked increases in exosomal miRNA-630 and miRNA-16–5p back to levels in healthy CO occurred in those children with OSA and ED after treatment (miRNA-630, pre-Tx -4.76 ± 0.97 vs. post-Tx 0.19 ± 0.32; n = 15; $P < 0.001$) (miRNA-16–5p, pre-Tx -2.87 ± 0.45 vs. post-Tx -0.87 ± 0.65; $P < 0.01$). The *in silico* putative targets of these five miRNAs are shown in Table E2.

Next, we extended our knowledge about the regulatory information network associated with the five miRNAs (*see* Figure E5), and found 24 regulatory information network validated targets: SPRYD4, PRDM13, ANK3, YIPF6, MEF2D, YTHDF1, SNAI2, CENTG2, KRT83, NPAS3, HEATR3, PRRT3, ATP1A1, BRPF3, TFAP2B, SET, RBM9, UBE2V1, C9orf39, RBM4, EPE300, MAP3K2, AP3B1, and CBX5.

miRNA-630 and Endothelial Function

To explore the putative function of miRNA cargo in the context of pediatric ED and as a proof of concept, we selected miRNA-630 as

the initial candidate based on the largest fold differences in expression between ED and NEF OS and children with OSA, and the largest responses in OSA_{ED} children after Tx. To this effect, specific miRNA-630 mimic and inhibitor were transfected into plasma-derived exosomes from ED and NEF, respectively (for control treatment, scrambled sequences of the mimic and inhibitor were used). Mimic-induced restoration of miRNA-630 content in ED-derived exosomes significantly ameliorated the adverse ED exosome-induced effects on ECIS measures of resistance across the endothelial cell monolayer and ZO-1 tight junction immunofluorescence in endothelial cells for both OB or children with OSA with ED (Figure 3), and also restored eNOS mRNA expression using control exosomes as reference (0.56 ± 0.17 in scrambled miRNA-treated endothelial cells vs. 0.94 ± 0.29 in mimic miRNA-treated endothelial cells; n = 4; $P < 0.05$). Conversely, transfection of NEF-derived exosomes with an miRNA-630 inhibitor was associated with disruption of the monolayer resistance and altered ZO-1 endothelial cell distribution (Figure 3), and reductions in eNOS expression in endothelial cells (0.47 ± 0.22 following treatment with miRNA-630 inhibitor vs. 1.04 ± 0.33 after scrambled miRNA; n = 5; $P < 0.02$).

miRNA-630 Gene Targets in Endothelial Cells

A schematic of the experimental subtraction-based approach for delineation of the miRNA-630 gene targets in human endothelial cells is shown in Figure 4. Using whole-genome transcriptomic analyses, a total of 416 gene targets were identified for miRNA-630 in endothelial cells, and correspond to 10 major canonical pathways (*see* Table E2). Notable among these pathways are, for example, NRF2-mediated oxidative stress responses, AMP kinase, and tight junction signaling pathways (Figure 4).

Discussion

This study shows that plasma exosomes from children with ED, either obese or suffering from OSA, induce marked *in vitro* and *in vivo* functional and structural alterations in endothelium that are mediated by altered exosomal miRNA cargo. Among the differentially expressed exosomal miRNAs, the expression of hsa-miR-630 was reduced, and emerged as a significant effector of ED. Restoration of hsa-miR-630 exosomal levels reverted the endothelial cell perturbations in ED-derived exosomes to control values, whereas inhibition of hsa-miR-630 in NEF-derived exosomes recapitulated the perturbations elicited by ED exosomal responses in endothelial cells. Taken together, we identify a microvesicle-based miRNA-mediated mechanism that is selectively altered in children who are at increased CVD risk.

In this study, in *a priori* different conditions (i.e., obesity and OSA), which are both associated with known increased risk for CVD (2, 6), and are further indistinguishable based on their lipid profile or systemic blood pressure measurements, we identified clear differences based on their postocclusive hyperemic responses (Table 1). The latter responses enable accurate reporting on the bioavailability of NO from eNOS sources in the circulation (31). Furthermore, incremental evidence attests to vascular remodeling that progressively occurs in the context of ED since early childhood to increase CVD risk later in life (32). The degree of eNOS expression changes in naive cultured endothelial cells treated with exosomes from ED or NEF subjects markedly differed, independently from whether the exosomes originated from OB without OSA or from non-OB with OSA (22). Additionally, changes in monolayer resistance were closely associated with T_{max}, suggesting that changes in eNOS expression and in monolayer resistance provide accurate biologic correlates of endothelial function *in vivo*. Furthermore, intravenous administration of equivalent doses of exosomes to otherwise healthy young mice generated markedly discrepant changes in postocclusive hyperemic responses in these animals that paralleled the original findings in children. These experiments strongly suggested that the circulating exosomes in children induce the vascular phenotype, and therefore prompted exploration of the exosomal cargo to identify potential candidates that may mediate the vascular deficits. However, because of the restricted amount of plasma available from any given child, we cannot deduce the specific contributions of exosomes from different cells sources to the *in vitro* or *in vivo* endothelial functional abnormalities.

Exosomes can perform intercellular transfer of miRNAs, thus participating in miRNA-based signaling (33, 34), and dysregulation of miRNA activity can lead to the development of a variety of diseases (35). There is increasing evidence that the effect of exosomes on target cells is mainly dependent on their intravesicular miRNA expression (36–38). Here, we found that fluorescently labeled exosomes were internalized into endothelial cells (*see* Figure E3), where they could be implicated in a myriad of important processes (39–44). Based on the selectivity of miRNA loading into extracellular vesicles (EV) and their stability (45), potential differences in miRNA exosomal cargo were identified, and were compatible with previous work implicating exosomal miRNAs not only in angiogenesis and other vascular phenomena (46, 47), while also suggesting the possibility that exosomes may provide therapeutic opportunities (48). We recently assessed the biomarker capabilities of plasma miRNAs (19), and our findings support the driving assumption that a cluster of circulating miRNAs may reliably discern between children with ED and

Figure 1. (Continued). curves of ECIS changes over time after administration of exosomes from control children (Co) and obese children with (OB_{ED}) and without (OB_{NEF}) endothelial dysfunction (n = 12/tracing; $P < 0.01$). (*C*) Ensemble-averaged curves of ECIS changes over time after administration of exosomes from control children (Co) and nonobese children with (OSA_{ED}) and without (OSA_{NEF}) endothelial dysfunction (n = 18/tracing; $P < 0.001$). (*D*) Effect of plasma exosomes on tight junction and adhesion molecule expression in naive endothelial cells. Representative images of at least six separate experiments show exosome-induced changes in expression of V-cadherin, zonula occludens (ZO)-1, intercellular adhesion molecule (ICAM)-1, and vascular cell adhesion molecule (VCAM)-1 in primary human endothelial cells after treatment with exosomes from obese children with endothelial dysfunction (OB_{ED}) and with normal endothelial function (OB_{NEF}). The *scale bars* for all the representative images are 25 μm. ED = endothelial dysfunction; NEF = normal endothelial function; T_{max} = time to maximal regional blood flow after occlusion release.

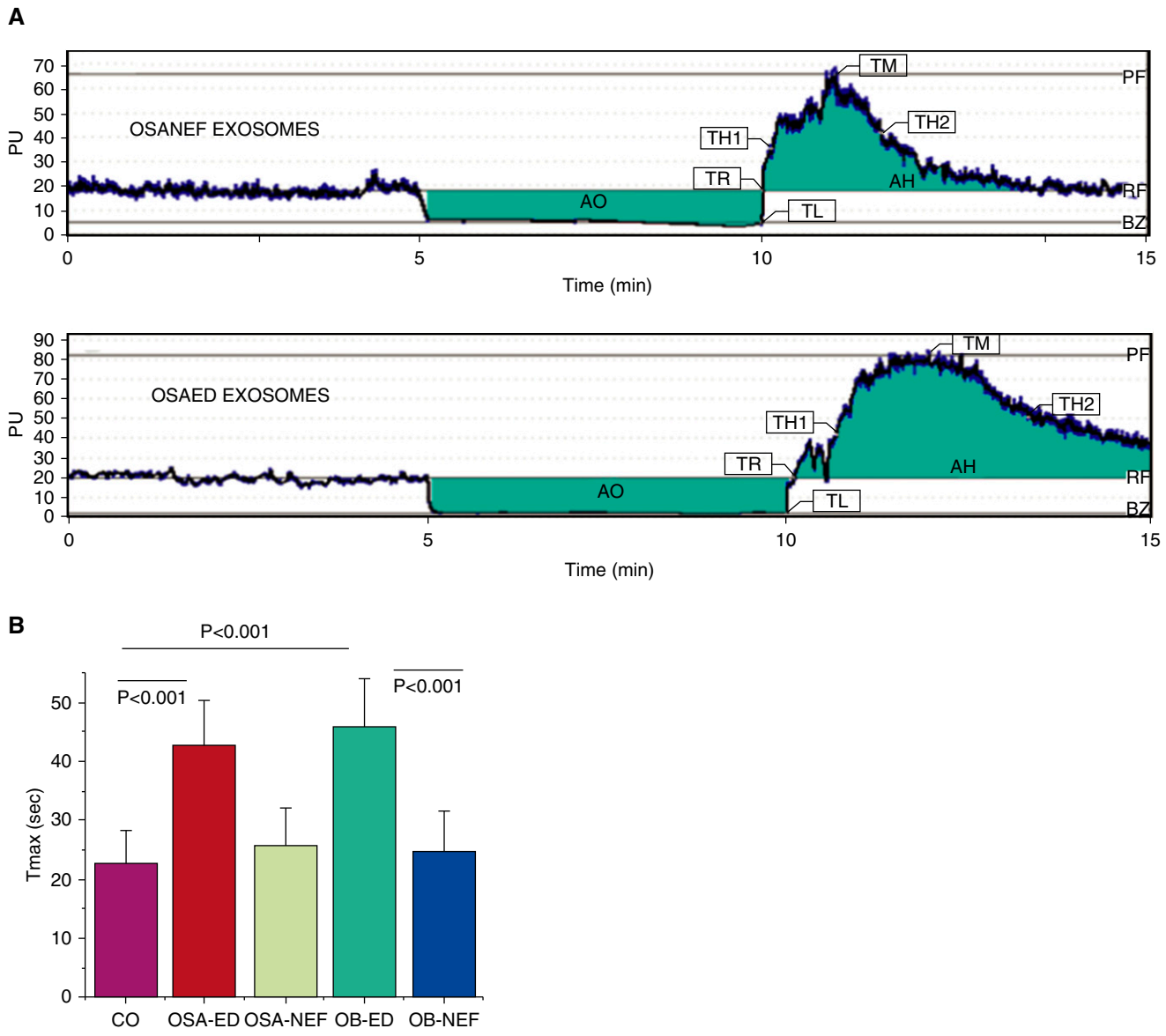

Figure 2. Exosome-mediated *in vivo* effects on vascular function in mice. (*A*) Typical examples of postocclusive reperfusion kinetics (5-min occlusion time) in a mouse injected once daily for 3 days with intravenous exosomes from a child with obstructive sleep apnea (OSA) and normal endothelial function (OSA_{NEF}) and in a mouse injected with exosomes from an age-, sex-, and body mass index *z* score–matched child with OSA with endothelial dysfunction (OSA_{ED}), illustrating the increased delay in time to peak reperfusion (T_{max}) in the mouse injected with ED-derived exosomes. (*B*) T_{max} values in mice injected with exosomes from control children (CO), OSA_{ED}, OSA_{NEF}, OB_{ED}, and OB_{NEF} (n = 8/group; *lines* indicate $P < 0.001$). AH = area of hyperemia; AO = arterial occlusion; BZ = basal zero; ED = endothelial dysfunction; NEF = normal endothelial function; OB = obese children; PF = peak flow; PU = perfusion units; RF = resting flow; TH1 = time to hyperemia 1; TH2 = time to hyperemia 2; TL = occlusion time lapsed; TM = time to maximal hyperemia; TR = time of release.

children with NEF. Among, the five differentially miRNAs identified through microarray approaches, a search of the literature revealed scarce information about these miRNAs regarding possible vascular targets (49). hsa-miR-630 was selected for further examination based on the prominent reduction in expression among children with ED, the marked increases in hsa-miR-630 in exosomes of children after treatment of OSA, and its previous association with angiogenesis and apoptotic processes in cancer (50, 51).

Here, we show that 24 regulatory information networks are affected when comparing ED with NEF (*see* Figure E5), and several of these genes were validated by RT-PCR in endothelial cells and play significant roles in preservation of endothelial cell integrity and functions. In addition, hsa-miR-16–5p has been implicated in cardiac cell functions in the context of heart failure, and identified in pericardial fluid (52). Based on the current consensus that miRNAs bind to their mRNA targets and induce their down-regulation, decreases in miRNA levels could then possibly be associated with increased expression of specific target genes and proteins. The experiments in which an miRNA-630 mimic and inhibitor were incorporated into exosomes enabled specific assessments of the functional

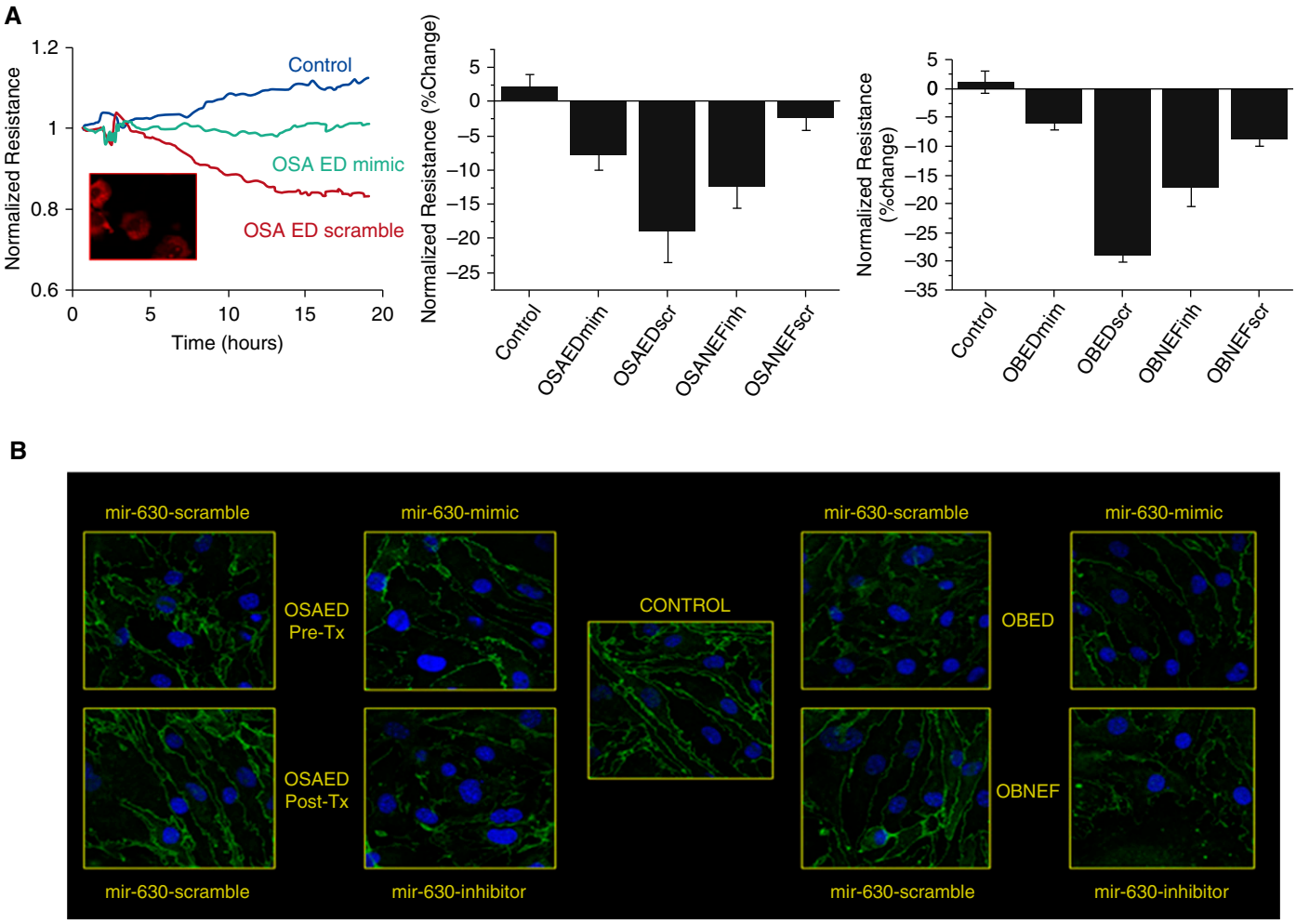

Figure 3. Effects of hsa-miR-630 mimic and inhibitor on endothelial dysfunction (ED) and normal endothelial function (NEF) plasma-derived exosome functional changes in endothelial cell monolayer resistance and tight junction protein expression (zonula occludens [ZO]-1). (*A*, *left*, *inset*) Representative image of plasma-derived immunofluorescently labeled exosomes after transfection with red fluorescence–labeled miRNA-630 mimic and administration to primary human endothelial cells. (*A*, *left*) Illustrative ensemble-averaged curves of endothelial cell monolayer resistance changes over time after administration of exosomes from six OSA_{ED} children treated with hsa-miR-630 mimic or scrambled mimic sequence against control empty exosomes. (*A*, *middle*) Summary of changes in normalized monolayer resistance measurements at 24 hours after treatment with control empty exosomes, exosomes from OSA_{ED} transfected with hsa-miR-630 mimic or scrambled mimic sequence, and exosomes from OSA_{NEF} children treated with miRNA-630 inhibitor or scrambled sequence (n = 8–12/experimental group). (*A*, *right*) Summary of changes in normalized monolayer resistance measurements at 24 hours after treatment with control empty exosomes, exosomes from OB_{ED} transfected with hsa-miR-630 mimic or scrambled mimic sequence, and exosomes from OB_{NEF} children treated with hsa-miR-630 inhibitor or scrambled sequence (n = 8–12/experimental group). (*B*) Representative images of at least six separate experiments showing exosome-induced changes in expression of ZO-1 in primary human endothelial cells after treatment with exosomes from obese children with (OB_{ED}) and without (OB_{NEF}) endothelial dysfunction, and from children with OSA and normal endothelial function (OSA_{NEF}) and age-, sex-, apnea–hypopnea index–, and body mass index *z* score–matched children with OSA and endothelial dysfunction (OSA_{ED}). Exosomes from subjects with ED were transfected with hsa-miR-630 mimic or scrambled mimic, whereas exosomes from subjects with NEF were transfected with hsa-miR-630 inhibitor or scrambled sequence as control. inh = inhibitor; mim = mimic; miRNA = microRNA; OB = obese; OSA = obstructive sleep apnea; scr = scrambled mimic; Tx = adenotonsillectomy.

role of miRNA-630 in endothelial cells, and confirmed the mechanistic role of this exosomal miRNA in the vasculature. Furthermore, transcriptomic strategies identified 416 gene targets for this miRNA in endothelium that clearly encompass well-established pathways in vascular homeostasis, such as Nrf2 (53, 54), AMP kinase pathways (55), and regulation of intercellular tight junctions (56–58).

Current findings further attest to the nondiscriminatory capacity of systemic blood pressure measurements or serum lipids in the detection of CVD risk, whereas endothelial functional measures either *in vivo* or *in vitro* enable demarcation between children with reduced or preserved NO bioavailability. Furthermore, we have identified an exosomal miRNA (i.e., miRNA-630) that not only recapitulates such findings but also enables functional restoration when delivered to endothelial cells. Thus, assessments of

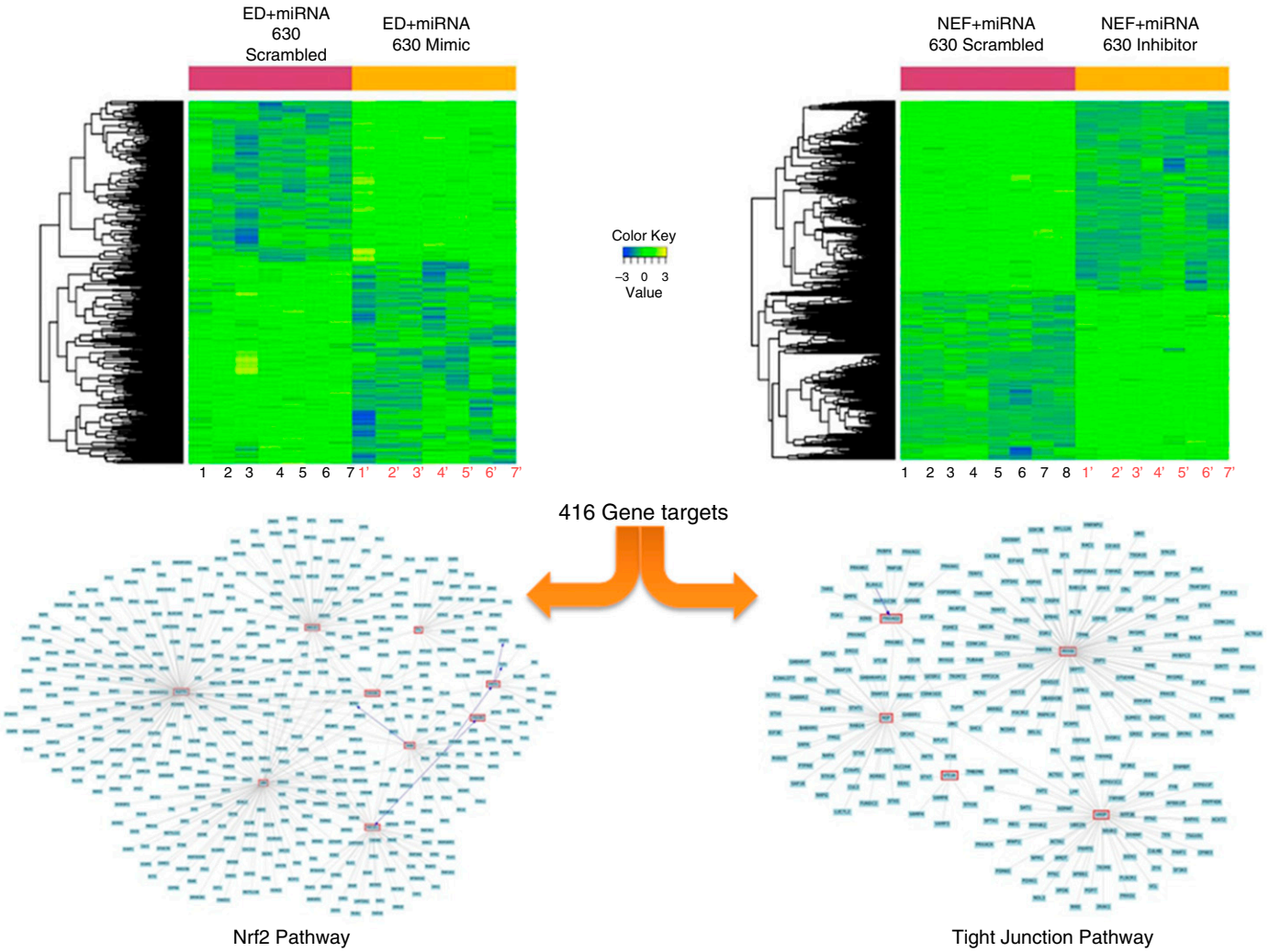

Figure 4. miRNA (hsa-miR-630) gene targets in human endothelial cells. *Left heatmap* depicts differentially expressed genes as determined via experiments comparing the effects of exosomes from seven children with endothelial dysfunction (ED) treated with either hsa-miR-630 mimic or control. *Right heatmap* shows differentially expressed genes as determined by experiments comparing the effects of exosomes of eight subjects with normal endothelial function (NEF) treated with hsa-miR-630 inhibitor and seven subjects with NEF treated with scrambled control. These experiments revealed a total of 416 gene targets in endothelial cells, corresponding to 10 major functional pathways, of which Nrf2 and tight junction pathways are shown for illustration purposes. Note that several of the putative hsa-miR-630 gene targets identified in the mRNA arrays were subsequently verified using reverse-transcriptase polymerase chain reaction strategies. miRNA = microRNA.

exosomal miRNA cargo may not only provide biomarkers to identify those children at risk for CVD later on, but may also permit development of therapeutic approaches aimed at restoring the appropriate expression and function of hsa-miR-630 endothelial cell targets that are essential for the regulation of various physiologic and pathologic processes in endothelium, including development, differentiation, and proliferation (59, 60). The selectivity of miRNA loading into EV and their stability (45) prompted our preferential search for potential differences in miRNA exosomal cargo using unbiased approaches, such as miRNA arrays. We believe that the ability to isolate exosomes and investigate their miRNA cargo would enable potential exploration as potential diagnostic, drug delivery, and drug target discovery tools for numerous human pathologies including CVD.

As with any study, we should highlight some limitations. First, the relatively restricted size of cohort of children studied will require additional studies in expanded cohorts to enable translation of the molecular miRNA signature into clinical practice. Second, the restricted quantities of plasma that were available from the participants were constrained by the bioethical committee, and precluded us from exploring differences in miRNA expression among specific cell-derived EV, and limited the quest for more extensive validation of all differentially expressed miRNAs for each and every one of the groups. Finally, the differences noted in BMI *z* scores between the OSA subgroups and between these groups and control subjects could signify that BMI may be a contributor to some of the exosome changes observed among patients with OSA, particularly those with ED.

In summary, we have shown that a dichotomous vascular outcome, such as the presence or absence of ED in pediatric OSA or in OB without OSA, as indicated by postocclusive hyperemic responses, can be recapitulated by *in vitro* or *in vivo* effects of plasma exosomes. Such exosome-induced alterations on naive endothelial cells or murine vascular responses can be explained, at least in part, by changes in miRNA-630 expression and its downstream coordinated effects on approximately 416 gene targets. Improved understanding of the mechanisms responsible for the differential individual vascular susceptibility to OSA or obesity in children should allow for improved delineation of CVD risk phenotypes, and for formulation of more individualized therapeutic strategies in those children at risk for future CVD. ■

Author disclosures are available with the text of this article at www.atsjournals.org.

References

1. Cote AT, Harris KC, Panagiotopoulos C, Sandor GG, Devlin AM. Childhood obesity and cardiovascular dysfunction. *J Am Coll Cardiol* 2013;62:1309–1319.
2. Hedvall Kallerman P, Hagman E, Edstedt Bonamy AK, Zemack H, Marcus C, Norman M, Westerståhl M. Obese children without comorbidities have impaired microvascular endothelial function. *Acta Paediatr* 2014;103:411–417.
3. McCrindle BW. Cardiovascular consequences of childhood obesity. *Can J Cardiol* 2015;31:124–130.
4. Amin RS, Kimball TR, Bean JA, Jeffries JL, Willging JP, Cotton RT, Witt SA, Glascock BJ, Daniels SR. Left ventricular hypertrophy and abnormal ventricular geometry in children and adolescents with obstructive sleep apnea. *Am J Respir Crit Care Med* 2002;165: 1395–1399.
5. Gozal D, Kheirandish-Gozal L, Serpero LD, Sans Capdevila O, Dayyat E. Obstructive sleep apnea and endothelial function in school-aged nonobese children: effect of adenotonsillectomy. *Circulation* 2007; 116:2307–2314.
6. Bhattacharjee R, Kheirandish-Gozal L, Pillar G, Gozal D. Cardiovascular complications of obstructive sleep apnea syndrome: evidence from children. *Prog Cardiovasc Dis* 2009;51:416–433.
7. Goldbart AD, Levitas A, Greenberg-Dotan S, Ben Shimol S, Broides A, Puterman M, Tal A. B-type natriuretic peptide and cardiovascular function in young children with obstructive sleep apnea. *Chest* 2010; 138:528–535.
8. Alonso-Álvarez ML, Cordero-Guevara JA, Terán-Santos J, Gonzalez-Martinez M, Jurado-Luque MJ, Corral-Peñafiel J, Duran-Cantolla J, Kheirandish-Gozal L, Gozal D. Obstructive sleep apnea in obese community-dwelling children: the NANOS study. *Sleep* 2014;37: 943–949.
9. Bhattacharjee R, Kim J, Alotaibi WH, Kheirandish-Gozal L, Capdevila OS, Gozal D. Endothelial dysfunction in children without hypertension: potential contributions of obesity and obstructive sleep apnea. *Chest* 2012;141:682–691.
10. Charakida M, Jones A, Falaschetti E, Khan T, Finer N, Sattar N, Hingorani A, Lawlor DA, Smith GD, Deanfield JE. Childhood obesity and vascular phenotypes: a population study. *J Am Coll Cardiol* 2012;60:2643–2650.
11. Bhattacharjee R, Alotaibi WH, Kheirandish-Gozal L, Capdevila OS, Gozal D. Endothelial dysfunction in obese non-hypertensive children without evidence of sleep disordered breathing. *BMC Pediatr* 2010;10:8.
12. Bhattacharjee R, Kim J, Kheirandish-Gozal L, Gozal D. Obesity and obstructive sleep apnea syndrome in children: a tale of inflammatory cascades. *Pediatr Pulmonol* 2011;46:313–323.
13. Li M, Rai AJ, DeCastro GJ, Zeringer E, Barta T, Magdaleno S, Setterquist R, Vlassov AV. An optimized procedure for exosome isolation and analysis using serum samples: application to cancer biomarker discovery. *Methods* 2015;87:26–30.
14. Rekker K, Saare M, Roost AM, Kubo AL, Zarovni N, Chiesi A, Salumets A, Peters M. Comparison of serum exosome isolation methods for microRNA profiling. *Clin Biochem* 2014;47:135–138.
15. Gozal D, Kheirandish-Gozal L, Bhattacharjee R, Spruyt K. Neurocognitive and endothelial dysfunction in children with obstructive sleep apnea. *Pediatrics* 2010;126:e1161–e1167.
16. Kourembanas S. Exosomes: vehicles of intercellular signaling, biomarkers, and vectors of cell therapy. *Annu Rev Physiol* 2015; 77:13–27.
17. Ribeiro MF, Zhu H, Millard RW, Fan GC. Exosomes function in pro- and anti-angiogenesis. *Curr Angiogenes* 2013;2:54–59.
18. Viaud S, Ploix S, Lapierre V, Théry C, Commere PH, Tramalloni D, Gorrichon K, Virault-Rocroy P, Tursz T, Lantz O, *et al*. Updated technology to produce highly immunogenic dendritic cell-derived exosomes of clinical grade: a critical role of interferon-γ. *J Immunother* 2011;34:65–75.
19. Khalyfa A, Gozal D. Exosomal miRNAs as potential biomarkers of cardiovascular risk in children. *J Transl Med* 2014;12:162.
20. Skog J, Würdinger T, van Rijn S, Meijer DH, Gainche L, Sena-Esteves M, Curry WT Jr, Carter BS, Krichevsky AM, Breakefield XO. Glioblastoma microvesicles transport RNA and proteins that promote tumour growth and provide diagnostic biomarkers. *Nat Cell Biol* 2008;10:1470–1476.
21. Valadi H, Ekström K, Bossios A, Sjöstrand M, Lee JJ, Lötvall JO. Exosome-mediated transfer of mRNAs and microRNAs is a novel mechanism of genetic exchange between cells. *Nat Cell Biol* 2007;9: 654–659.
22. Kheirandish-Gozal L, Khalyfa A, Gozal D, Bhattacharjee R, Wang Y. Endothelial dysfunction in children with obstructive sleep apnea is associated with epigenetic changes in the eNOS gene. *Chest* 2013; 143:971–977.
23. Keese CR, Bhawe K, Wegener J, Giaever I. Real-time impedance assay to follow the invasive activities of metastatic cells in culture. *Biotechniques* 2002;33:842–844, 846, 848–850.
24. Rahim S, Üren A. A real-time electrical impedance based technique to measure invasion of endothelial cell monolayer by cancer cells. *J Vis Exp* 2011;50:2792.
25. Kutmon M, Kelder T, Mandaviya P, Evelo CT, Coort SL. CyTargetLinker: a cytoscape app to integrate regulatory interactions in network analysis. *PLoS One* 2013;8:e82160.
26. Shannon P, Markiel A, Ozier O, Baliga NS, Wang JT, Ramage D, Amin N, Schwikowski B, Ideker T. Cytoscape: a software environment for integrated models of biomolecular interaction networks. *Genome Res* 2003;13:2498–2504.
27. Ong SG, Lee WH, Huang M, Dey D, Kodo K, Sanchez-Freire V, Gold JD, Wu JC. Cross talk of combined gene and cell therapy in ischemic heart disease: role of exosomal microRNA transfer. *Circulation* 2014; 130(Suppl 1):S60–S69.
28. Raff U, Ott C, John S, Schmidt BM, Fleischmann EH, Schmieder RE. Nitric oxide and reactive hyperemia: role of location and duration of ischemia. *Am J Hypertens* 2010;23:865–869.
29. Simons M, Raposo G. Exosomes: vesicular carriers for intercellular communication. *Curr Opin Cell Biol* 2009;21:575–581.
30. Théry C. Exosomes: secreted vesicles and intercellular communications. *F1000 Biol Rep* 2011;3:15.
31. Visentin S, Grumolato F, Nardelli GB, Di Camillo B, Grisan E, Cosmi E. Early origins of adult disease: low birth weight and vascular remodeling. *Atherosclerosis* 2014;237:391–399.
32. Fernandez-Messina L, Gutierrez-Vazquez C, Rivas-Garcia E, Sanchez-Madrid F, de la Fuente H. Immunomodulatory role of micrornas transferred by extracellular vesicles. *Biol Cell* 2015;107:61–77.
33. Kosaka N, Iguchi H, Yoshioka Y, Takeshita F, Matsuki Y, Ochiya T. Secretory mechanisms and intercellular transfer of microRNAs in living cells. *J Biol Chem* 2010;285:17442–17452.
34. Carrington JC, Ambros V. Role of microRNAs in plant and animal development. *Science* 2003;301:336–338.
35. Croce CM. Causes and consequences of microRNA dysregulation in cancer. *Nat Rev Genet* 2009;10:704–714.

36. Cantaluppi V, Gatti S, Medica D, Figliolini F, Bruno S, Deregibus MC, Sordi A, Biancone L, Tetta C, Camussi G. Microvesicles derived from endothelial progenitor cells protect the kidney from ischemia-reperfusion injury by microRNA-dependent reprogramming of resident renal cells. *Kidney Int* 2012;82:412–427.
37. Diehl P, Fricke A, Sander L, Stamm J, Bassler N, Htun N, Ziemann M, Helbing T, El-Osta A, Jowett JB, *et al*. Microparticles: major transport vehicles for distinct microRNAs in circulation. *Cardiovasc Res* 2012; 93:633–644.
38. Loyer X, Vion AC, Tedgui A, Boulanger CM. Microvesicles as cell-cell messengers in cardiovascular diseases. *Circ Res* 2014;114:345–353.
39. Lo Cicero A, Stahl PD, Raposo G. Extracellular vesicles shuffling intercellular messages: for good or for bad. *Curr Opin Cell Biol* 2015; 35:69–77.
40. Lässer C. Exosomes in diagnostic and therapeutic applications: biomarker, vaccine and RNA interference delivery vehicle. *Expert Opin Biol Ther* 2015;15:103–117.
41. Colombo M, Raposo G, Théry C. Biogenesis, secretion, and intercellular interactions of exosomes and other extracellular vesicles. *Annu Rev Cell Dev Biol* 2014;30:255–289.
42. Tian T, Wang Y, Wang H, Zhu Z, Xiao Z. Visualizing of the cellular uptake and intracellular trafficking of exosomes by live-cell microscopy. *J Cell Biochem* 2010;111:488–496.
43. Gajos-Michniewicz A, Duechler M, Czyz M. MiRNA in melanoma-derived exosomes. *Cancer Lett* 2014;347:29–37.
44. Wiklander OP, Nordin JZ, O'Loughlin A, Gustafsson Y, Corso G, Mäger I, Vader P, Lee Y, Sork H, Seow Y, *et al*. Extracellular vesicle in vivo biodistribution is determined by cell source, route of administration and targeting. *J Extracell Vesicles* 2015;4:26316.
45. Mitchell PS, Parkin RK, Kroh EM, Fritz BR, Wyman SK, Pogosova-Agadjanyan EL, Peterson A, Noteboom J, O'Briant KC, Allen A, *et al*. Circulating microRNAs as stable blood-based markers for cancer detection. *Proc Natl Acad Sci USA* 2008;105:10513–10518.
46. Finn NA, Searles CD. Intracellular and extracellular miRNAs in regulation of angiogenesis signaling. *Curr Angiogenes* 2012;4: 299–307.
47. Katoh M. Therapeutics targeting angiogenesis: genetics and epigenetics, extracellular miRNAs and signaling networks [review]. *Int J Mol Med* 2013;32:763–767.
48. Schober A, Nazari-Jahantigh M, Weber C. MicroRNA-mediated mechanisms of the cellular stress response in atherosclerosis. *Nat Rev Cardiol* 2015;12:361–374.
49. Galluzzi L, Morselli E, Vitale I, Kepp O, Senovilla L, Criollo A, Servant N, Paccard C, Hupé P, Robert T, *et al*. miR-181a and miR-630 regulate cisplatin-induced cancer cell death. *Cancer Res* 2010;70:1793–1803.
50. Kuo TC, Tan CT, Chang YW, Hong CC, Lee WJ, Chen MW, Jeng YM, Chiou J, Yu P, Chen PS, *et al*. Angiopoietin-like protein 1 suppresses SLUG to inhibit cancer cell motility. *J Clin Invest* 2013;123: 1082–1095.
51. Kuosmanen SM, Hartikainen J, Hippeläinen M, Kokki H, Levonen AL, Tavi P. MicroRNA profiling of pericardial fluid samples from patients with heart failure. *PLoS One* 2015;10:e0119646.
52. Wei Y, Gong J, Thimmulappa RK, Kosmider B, Biswal S, Duh EJ. Nrf2 acts cell-autonomously in endothelium to regulate tip cell formation and vascular branching. *Proc Natl Acad Sci USA* 2013;110: E3910–E3918.
53. Ramprasath T, Vasudevan V, Sasikumar S, Puhari SS, Saso L, Selvam GS. Regression of oxidative stress by targeting eNOS and Nrf2/ARE signaling: a guided drug target for cardiovascular diseases. *Curr Top Med Chem* 2015;15:857–871.
54. Kurokawa H, Sugiyama S, Nozaki T, Sugamura K, Toyama K, Matsubara J, Fujisue K, Ohba K, Maeda H, Konishi M, *et al*. Telmisartan enhances mitochondrial activity and alters cellular functions in human coronary artery endothelial cells via AMP-activated protein kinase pathway. *Atherosclerosis* 2015;239:375–385.
55. Kao CH, Chen JK, Yang VC. Ultrastructure and permeability of endothelial cells in branched regions of rat arteries. *Atherosclerosis* 1994;105:97–114.
56. Krouwer VJ, Hekking LH, Langelaar-Makkinje M, Regan-Klapisz E, Post JA. Endothelial cell senescence is associated with disrupted cell-cell junctions and increased monolayer permeability. *Vasc Cell* 2012;4:12.
57. Bian C, Xu G, Wang J, Ma J, Xiang M, Chen P. Hypercholesterolaemic serum increases the permeability of endothelial cells through zonula occludens-1 with phosphatidylinositol 3-kinase signaling pathway. *J Biomed Biotechnol* 2009;2009:814979.
58. Foteinos G, Hu Y, Xiao Q, Metzler B, Xu Q. Rapid endothelial turnover in atherosclerosis-prone areas coincides with stem cell repair in apolipoprotein E-deficient mice. *Circulation* 2008;117:1856–1863.
59. Zhang C. MicroRNAs in vascular biology and vascular disease. *J Cardiovasc Transl Res* 2010;3:235–240.
60. Pigati L, Yaddanapudi SC, Iyengar R, Kim DJ, Hearn SA, Danforth D, Hastings ML, Duelli DM. Selective release of microRNA species from normal and malignant mammary epithelial cells. *PLoS One* 2010;5: e13515.